Received: 1 March 2021 | Revised: 1 August 2021 | Accepted: 2 August 2021

DOI: 10.1002/dvg.23442

RESEARCH ARTICLE

genesis WILEY

Targeted deletion of *Atoh8* results in severe hearing loss in mice

Qi Tang[1,2] | Meng-Yao Xie[1,2] | Yong-Li Zhang[1,2] | Ruo-Yan Xue[1,2] | Xiao-Hui Zhu[1,2] | Hua Yang[1,2]

[1]Department of Otolaryngology, Peking Union Medical College Hospital, Chinese Academy of Medical Sciences and Peking Union Medical College, Beijing, China

[2]Translational Medicine Center, Peking Union Medical College Hospital, Chinese Academy of Medical Sciences and Peking Union Medical College, Beijing, China

Correspondence
Hua Yang, Department of Otolaryngology, Peking Union Medical College Hospital, No. 1 Shuaifuyuan, Dongcheng District, Beijing, 100730, China.
Email: dr_yanghua2021@163.com

Funding information
The Scientific Project of Young and Middle-aged Researcher of PUMCH, Grant/Award Number: pumch-2013-007; Scientific Project of Young and Middle-aged Researchers of PUMCH, Grant/Award Number: pumch-2013-007; Beijing Natural Science Foundation, Grant/Award Number: 7172176; National Natural Science Foundation of China, Grant/Award Number: 81470698

Summary

Atoh8, also named *Math6*, is a bHLH gene reported to have important functions in the developing nervous system, pancreas and kidney. However, the expression pattern and function of Atoh8 in the inner ear are still unclear. To study the function of Atoh8 in the developing mouse inner ear, we performed targeted deletion of *Atoh8* by intercrossing *Atoh8*$^{lacZ/+}$ mice. We studied the expression pattern of *Atoh8* in the inner ear and found interesting results that *Atoh8*-null (*Atoh8*$^{lacZ/lacZ}$) mice were viable but smaller than their littermates and they were severely hearing impaired, which was confirmed by hearing tests (ABR, DPOAE). We collected 129 viable newborns from 18 litters by crossing *Atoh8*$^{lacZ/+}$ mice and found that the distributions of *Atoh8*$^{lacZ/+}$, *Atoh8*$^{lacZ/lacZ}$ and wild type were very close to their expected Mendelian ratio by χ^2 testing. However, no remarkable morphological changes in cochleae in mutant mice were detected under plastic sectioning and electron microscopy. No remarkable differences in the expression of Myosin6, Prestin, TrkC, GAD65, Tuj1, or Calretinin were detected between the mutant mice and the control mice. These findings indicate that *Atoh8* plays an important role in the development of normal hearing, while further studies are required to elucidate its exact function in hearing.

KEYWORDS
Atoh8, hearing loss, mice, targeted deletion

1 | INTRODUCTION

Atoh8, also named Math6, is a bHLH gene expressed in the developing nervous system (Inoue et al., 2001), pancreas (Lynn, Sanchez, Gomis, German, & Gasa, 2008), vertebra (Rawnsley et al., 2013), and kidney (Ross et al., 2006). As a mammalian homolog of the proneural gene *atonal* in *Drosophila*, *Atoh8* shows uniqueness because there are three exons in its coding region, while other atonal homologs have only a single exon in their coding regions (Ejarque, Altirriba, Gomis, & Gasa, 2013; Inoue et al., 2001). Atoh8 has been detected in both neuronal precursor cells and mature neurons (Inoue et al., 2001; Wang, Balakrishnan-Renuka, Napirei, Theiss, & Brand-Saberi, 2015). Atoh8 was also shown to be expressed in the metanephric mesenchyme in the early developmental stage of the kidney and later was restrictively expressed in podocytes in the adult kidney (Chen et al., 2016; Ross et al., 2006). Atoh8 was identified as a novel transcription factor that plays an essential role in the embryonic development of the pancreas and functions downstream of Neurog3 (Lynn et al., 2008). The Atoh8 mutant allele may cause early embryonic lethality (Ejarque

Qi Tang and Meng-Yao Xie have contributed equally to this study.

et al., 2016; Lynn et al., 2008). However, the expression pattern and function of Atoh8 in the inner ear are still unclear.

The mammalian inner ear is a complicated organ that is composed of two parts: the cochlea and the vestibule. The cochlea is responsible for hearing and the vestibule functions in balance and the detection of acceleration and deceleration. Normal development of the inner ear depends on the synchronized functions of multiple genes, including *Fgf3*, *Fgf10* (Alvarez et al., 2003; Wright & Mansour, 2003), *BMP4* (Li et al., 2005), *Sox2* (Kiernan et al., 2005; Oesterle, Campbell, Taylor, Forge, & Hume, 2008) and bHLH genes, including *Neurog1* (Matei et al., 2005), *NeuroD1* (Kim et al., 2001), *Math1* (Bermingham et al., 1999; Chen, Johnson, Zoghbi, & Segil, 2002; Raft et al., 2007; Zhang et al., 2018), and *GATA3* (Lawoko-Kerali et al., 2004). To clarify the function of Atoh8 in the development of the mammalian inner ear, we studied the expression pattern of Atoh8 in the developing mouse inner ear and its function by targeted deletion of *Atoh8*. Our study showed that *Atoh8*-null (*Atoh8*$^{lacZ/lacZ}$) mice were viable but severely hearing impaired. This finding indicates that Atoh8 plays an important role in the development of normal hearing.

2 | RESULTS

2.1 | Generation of the *Atoh8-lacZ* knock-in mouse line

We obtained *Atoh8*$^{lacZ/+}$ mice from Dr. Lin Gan. We generated the targeted deletion of *Atoh8* by intercrossing *Atoh8*$^{lacZ/+}$ mice. The *Atoh8-lacZ* mouse line was generated by Dr. Lin Gan by removing the coding sequences from exon 1 of *Atoh8*, including the translational initiation codon, and placing *lacZ* under the control of the *atoh8* regulatory sequences (Figure 1a). The targeted event of the *Atoh8-lacZ* mice was confirmed by using a 5′ Southern probe to identify 5.6 kb wild-type (black arrow, Figure 1b) and 10.2 kb targeted (open arrow, Figure 1b) DNA fragments from BamHI-digested genomic DNA (Figure 1b). PCR genotyping was performed to determine the wild-type allele (482 bp, black arrow, Figure 1c) and the *Atoh8-lacZ* allele (900 bp, open arrow, Figure 1c). RT-qPCR showed the absence of *Atoh8* mRNA transcription in the inner ear, eye and kidney in the mutant (*Atoh8*$^{lacZ/lacZ}$) mice compared to the control mice (*Atoh8*$^{lacZ/+}$) at P5 (Figure 1d).

2.2 | *Atoh8*$^{lacZ/lacZ}$ mice are viable but smaller than their littermates

Similar to the heterozygous Atoh8$^{+/EGFP\text{-}Cre}$ mice reported previously (Lynn et al., 2008), the heterozygous Atoh8$^{lacZ/+}$ mice were viable and fertile and displayed no discernible defects. Previous studies also showed that mutant mice obtained by intercrossing heterozygous Atoh8$^{+/EGFP\text{-}Cre}$ mice were early embryonic lethal (Lynn et al., 2008). However, the Atoh8$^{lacZ/lacZ}$ mice we generated were viable and fertile. We collected 129 viable newborns from 18 litters by crossing Atoh8$^{lacZ/+}$ mice and found that the distributions of Atoh8$^{lacZ/+}$, Atoh8$^{lacZ/lacZ}$ and wide type were very close to their expected Mendelian ratios by $\chi 2$ testing (Figure 2a, $\chi^2 = 0.777$, $v = 2.00$, $p = .505$).

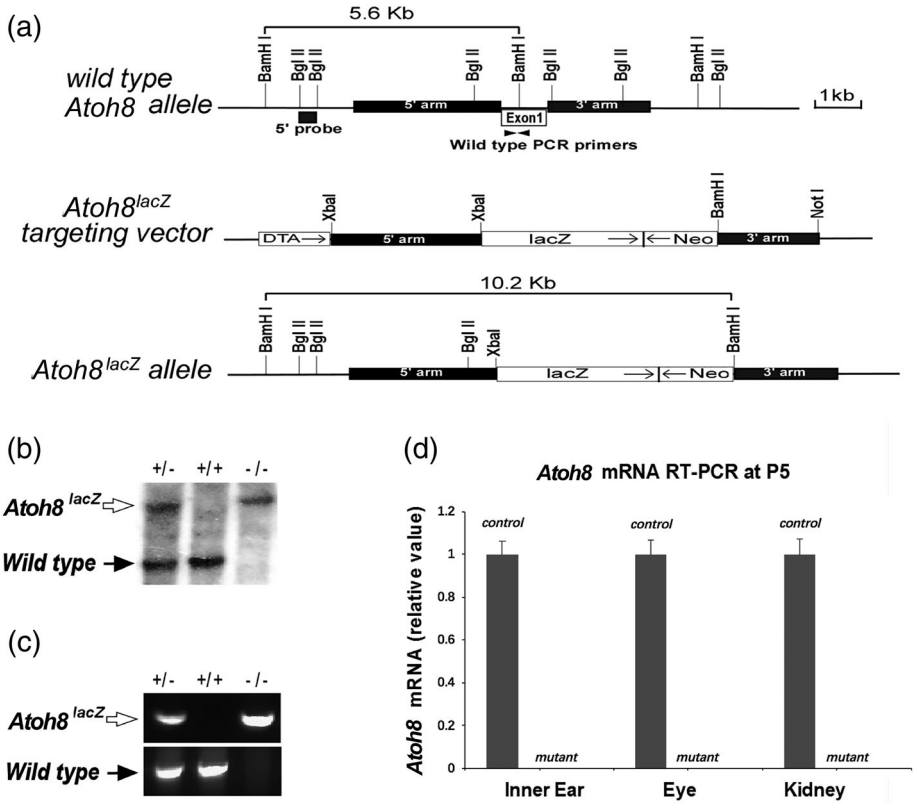

FIGURE 1 Generation of the *Atoh8-lacZ* knock-in mouse line. (a) Generation of the *Atoh8-lacZ* mouse line by removing the coding sequences from exon 1 of *Atoh8*, including the translational initiation codon, and placing *lacZ* under the control of *Atoh8* regulatory sequences. (b) The targeted event of the *Atoh8-lacZ* mice was confirmed by using a 5′ Southern probe to identify 5.6 kb wild-type (black arrow) and 10.2 kb targeted (open arrow) DNA fragments from BamHI-digested genomic DNA. (c) PCR genotyping was performed to determine the wild-type allele (482 bp, black arrow) and the *Atoh8-lacZ* allele (900 bp, open arrow). D: RTPCR showed the absence of *Atoh8* mRNA transcription in the inner ear, eye and kidney in the mutant (*Atoh8*$^{lacZ/lacZ}$) mice compared to the control mice (*Atoh*$^{8lacZ/+}$) at P5

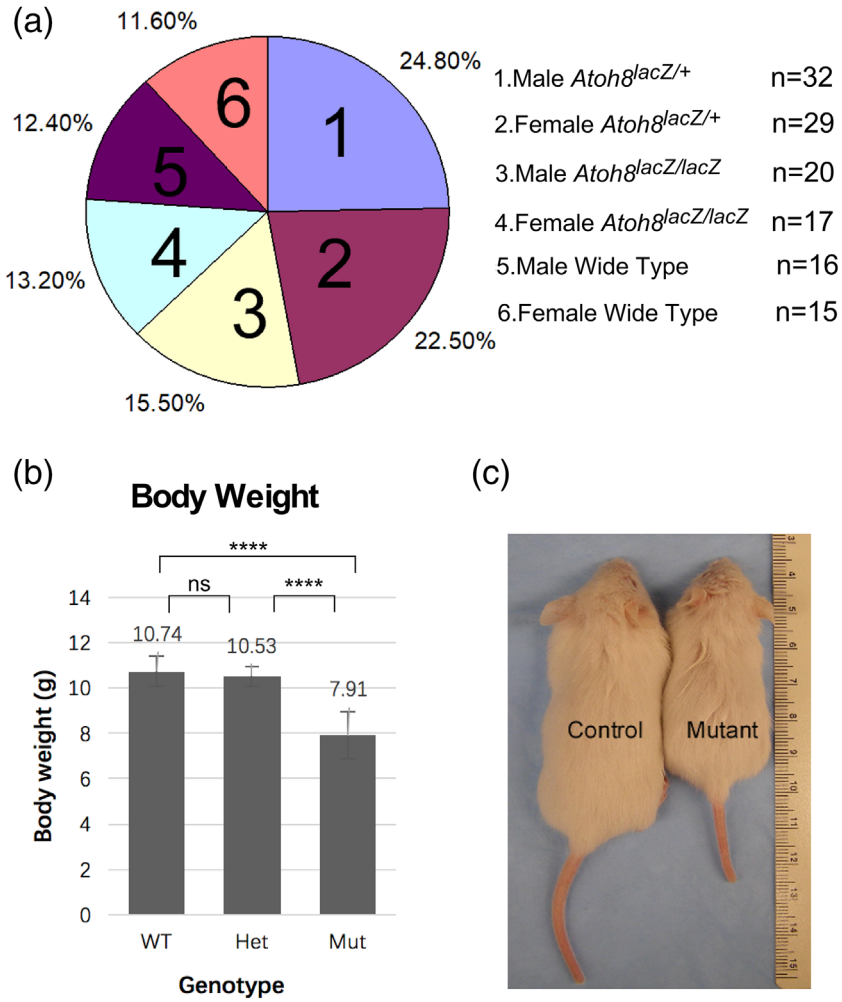

FIGURE 2 Distribution of different genotypes and the comparison of body weights. (a) A total of 129 viable newborns from 18 litters from the crossing of $Atoh^{8lacZ/+}$ mice were collected, and the distributions of $Atoh8^{lacZ/+}$, $Atoh^{8lacZ/lacZ}$ and wide type were very close to their expected Mendelian ratios by $\chi 2$ testing. (b,c) The differences in body weight between control (wild-type and heterozygous) mice and *Atoh8* mutant mice were statistically significant. The differences in body weights were not statistically significant between the heterozygotic and wild-type mice. ns: no significance, ****$p < .0001$

We also found that many of the mutant mice were visibly smaller than their littermates (Figure 2c). The differences in body weight between wild-type mice and Atoh8 mutant mice were statistically significant (*t* test, $p = 3.21E\text{-}05$), and the differences in body weight between heterozygous mice and Atoh8 mutant mice were statistically significant (*t* test, $p = 9.17E\text{-}05$). The differences in body weights were not statistically significant between the heterozygotic and wild-type mice (*t* test, $p = .43$).

2.3 | $Atoh8^{lacZ/lacZ}$ mice are hearing impaired

The mutant mice showed a poor response to the auricle response, so we tested their hearing by ABR and DPOAE. Hearing tests showed that $Atoh8^{lacZ/lacZ}$ mice were severely hearing impaired (Figure 3). The ABR results showed that the hearing thresholds of the mutant mice at frequencies of 8, 12, 16, and 32 kHz were significantly increased compared to those of the control mice (Figure 3a). DPOAE measurements also showed that thresholds were significantly increased in mutant mice compared to control mice (Figure 3b). Both ABR and DPOAE measurements indicated that mutant mice were severely hearing impaired. We did not find any symptoms of vestibular dysfunction in mutant or heterozygotic mice.

2.4 | *Atoh8* expression pattern

To clarify the expression pattern of Atoh8, we first detected its expression at early embryonic stages by X-gal staining in $Atoh8^{lacZ/+}$ mice (Figure 4). Compared to the wild-type mice, $Atoh8^{lacZ/+}$ mice showed *LacZ* signals at the developing inner ear at E10.5, E12.5 and E14.5 (Figure 4b,c,f, black arrows). *LacZ* signals were also detected at pod buds (Figure 4b, white arrowheads), vertebrae (Figure 4b,c,f, black arrowheads), the brain and heart (Figure 4c, black arrow and asterisk), whiskers (Figure 4e, black asterisk) and maniphalanx (Figure 4e, black arrowhead).

In the developing cochlea at later embryonic stages (E16.5–E18.5), Atoh8 expression was detected mainly in spiral ganglion neurons (Figure 5, asterisks), inner and outer cochlear hair cells (Figure 5, HC), Kölliker's organ (Figure 5, KO), supporting cells lateral to hair cells (Figure 5, SC), the stria vascularis (Figure 5, SV) and the cochlear bony covering (Figure 5). We used samples treated with a secondary antibody only as a blank control and did not detect lacZ or TUJ1 signals in control samples.

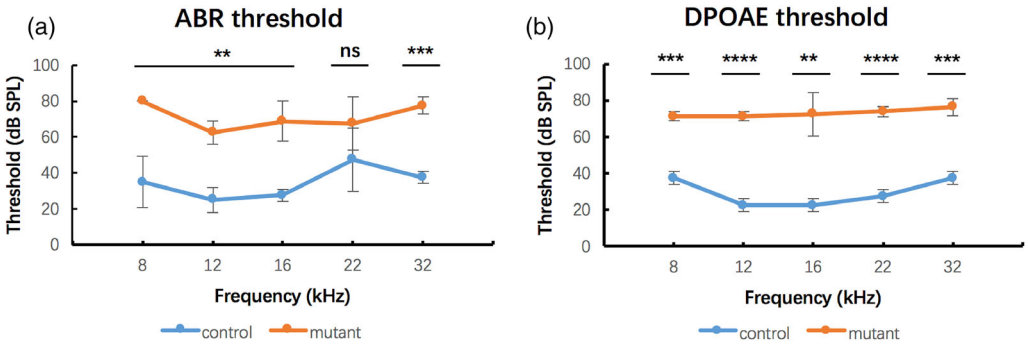

FIGURE 3 Hearing tests of *Atoh8* control and mutant mice. Hearing tests showed that *Atoh*$^{8lacZ/lacZ}$ mice were severely hearing impaired. (a) ABR results show hearing thresholds of the mutant mice at frequencies of 8, 12, 16, 22, and 32 kHz are significantly increased compared to that of the control mice. (b) DPOAE measurements also show that thresholds are significantly increased in mutant mice compared to control mice. age: P21, ns, no significance, $^{**}p < .01$, $^{***}p < .001$, $^{****}p < .0001$

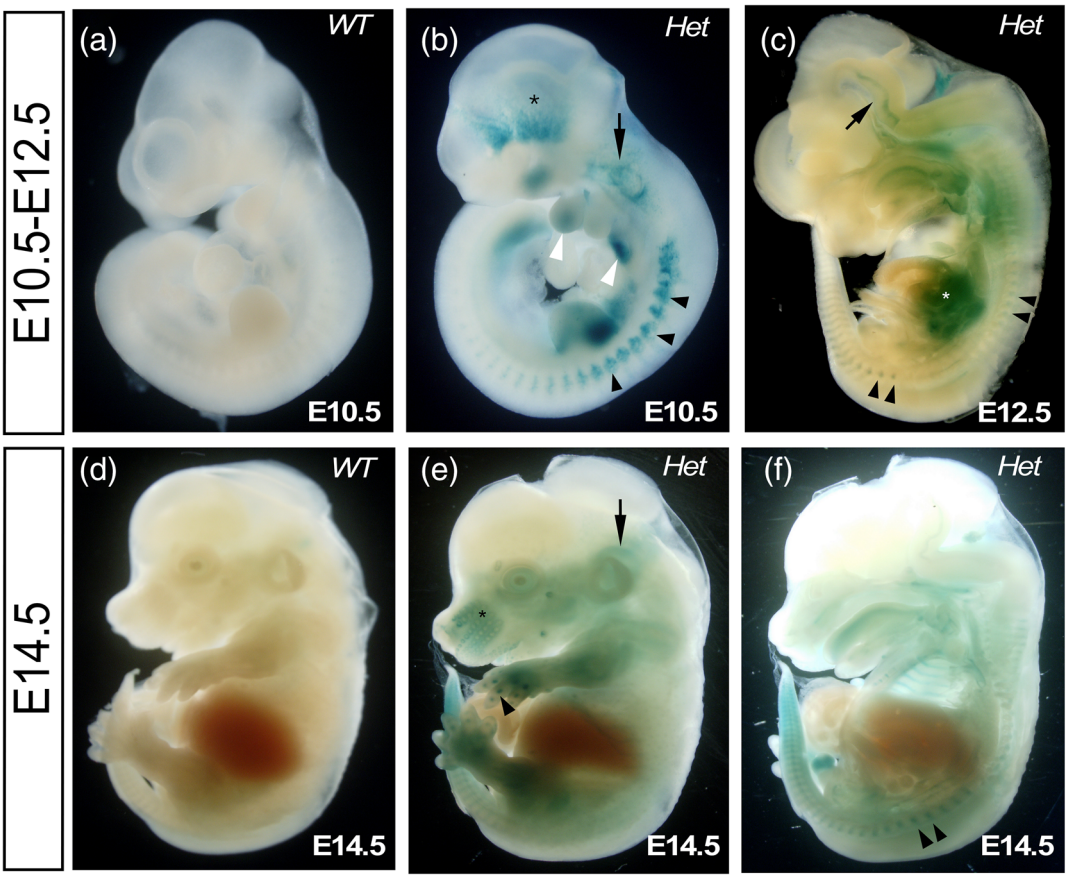

FIGURE 4 Expression pattern of Atoh8 at early embryonic stages by X-gal staining. Compared to the wild-type mice, *Atoh8*$^{lacZ/+}$ mice showed LacZ signals in the developing inner ear at E10.5, E12.5, and E14.5 (b,c,f, black arrows). LacZ signals were also detected at pod buds (b, white arrowheads), vertebrae (b,c,f, black arrowheads), the brain and heart (c, black arrow and asterisk), whiskers (e, black asterisk) and maniphalanx (e, black arrowhead)

2.5 | Cochlear morphology and structure in *Atoh8*$^{lacZ/lacZ}$ mice

The immunostaining data shown above suggest that Atoh8 is expressed at multiple structures inside the cochlea, including spiral ganglion cells, hair cells, supporting cells, Kölliker's organ and the stria vascularis, which may be potential sites causing hearing loss with variable severity. Therefore, we studied the morphology and structure of the cochlea of wild-type and *Atoh8*$^{lacZ/lacZ}$ mice. First, we checked several markers expressed in normal spiral ganglion cells, hair cells

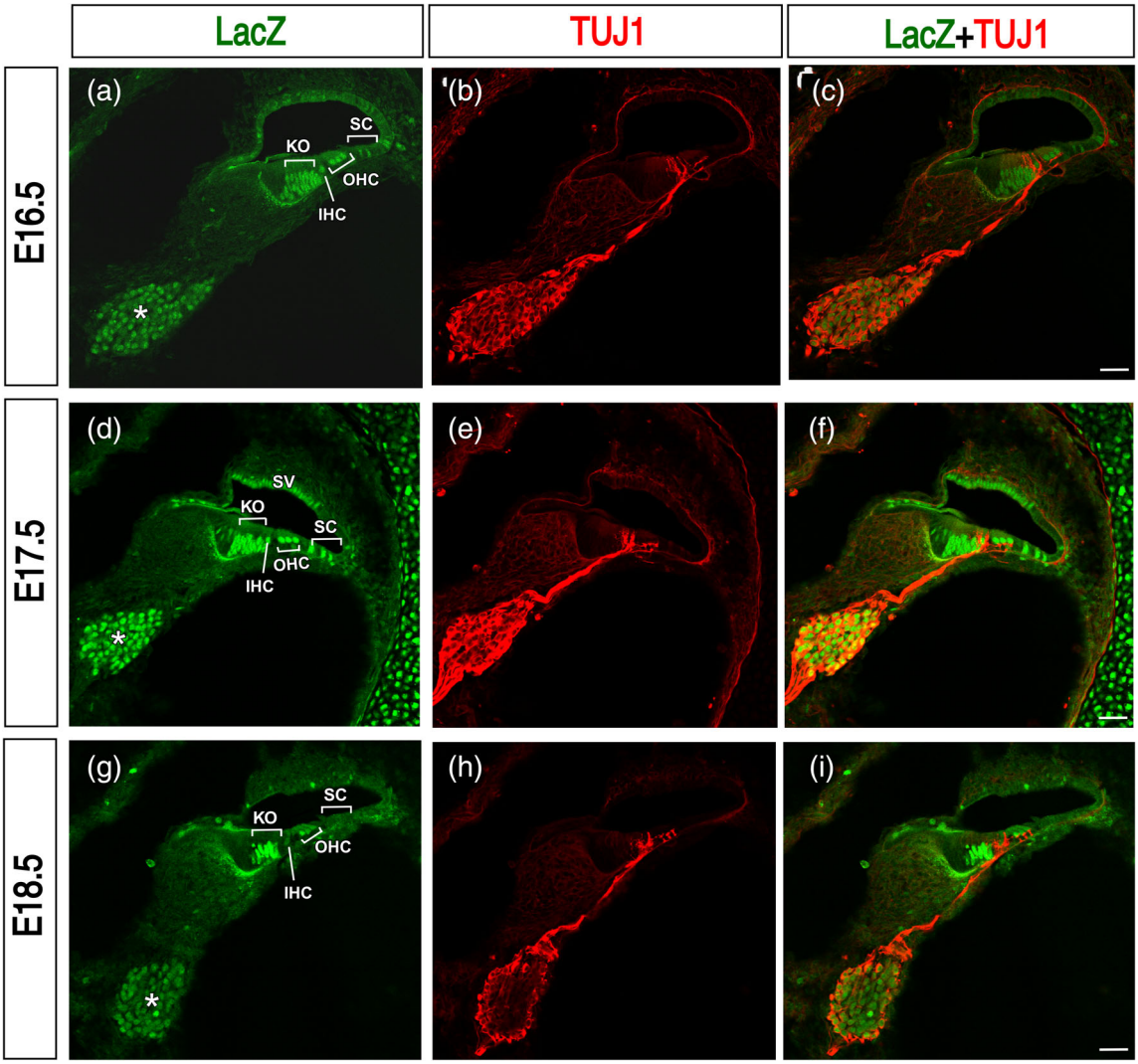

FIGURE 5 Expression pattern of Atoh8 at later embryonic stages by immunostaining. At E16.5–E18.5, Atoh8 expression was detected mainly in spiral ganglion neurons (asterisks), inner and outer cochlear hair cells (HC), Kölliker's organ (KO), supporting cells lateral to hair cells (SC), the stria vascularis (SV), and the cochlear bony covering

and/or supporting cells. At later embryonic and adult stages, Myosin6, a marker of mature hair cells, was clearly visible in both control mouse and *Atoh8*$^{lacZ/lacZ}$ mouse cochleae (Figure 6). PRESTIN, a marker specific for outer hair cells, was also strongly expressed in both control and mutant mice (Figure 6). There seemed to be no obvious difference in the expression of TrkC, GAD65, Tuj1, or Calretinin between wild-type and mutant mice (Figure 6).

Furthermore, we checked the morphology of mutant mouse cochleae by plastic sectioning and scanning electron microscopy (EM). We did not find any obvious abnormalities in cochlear morphology, spiral ganglion cells, the organ of Corti or the tectorial membrane of mutant mice when compared with those of control mice under a light microscope (Figure 7a–h). We further observed cochlear samples by scanning EM. Under scanning EM, the cilia of the inner and outer hair cells of mutant mice were clear and seemed normal compared with those of the control mice (Figure 7i,j).

3 | DISCUSSION

3.1 | *Atoh8*$^{lacZ/lacZ}$ mice are viable and fertile

Atoh8 (Math6) is a member of *Atoh* family (Inoue et al., 2001; Lynn et al., 2008; Ross et al., 2006). *Math1 (Atoh1)* and *Math5 (Atoh7)*, two other important members of the *Atoh* family, have been confirmed to play essential roles in the development of the inner ear (Bermingham et al., 1999; Chen et al., 2002; Fritzsch et al., 2005; Jahan, Pan, Kersigo, & Fritzsch, 2010) and retina (Feng et al., 2010; Wang et al., 2001; Yang, Ding, Pan, Deng, & Gan, 2003), respectively. Atoh8 is reported to play essential roles in the development of the skeletal muscle and retina of zebrafish (Place & Smith, 2017; Yao et al., 2010) in addition to its function in the pancreas, kidney and neurons (Inoue et al., 2001; Lynn et al., 2008; Ross et al., 2006; Wang et al., 2016; Yao et al., 2010). Therefore, we wanted to study the function of

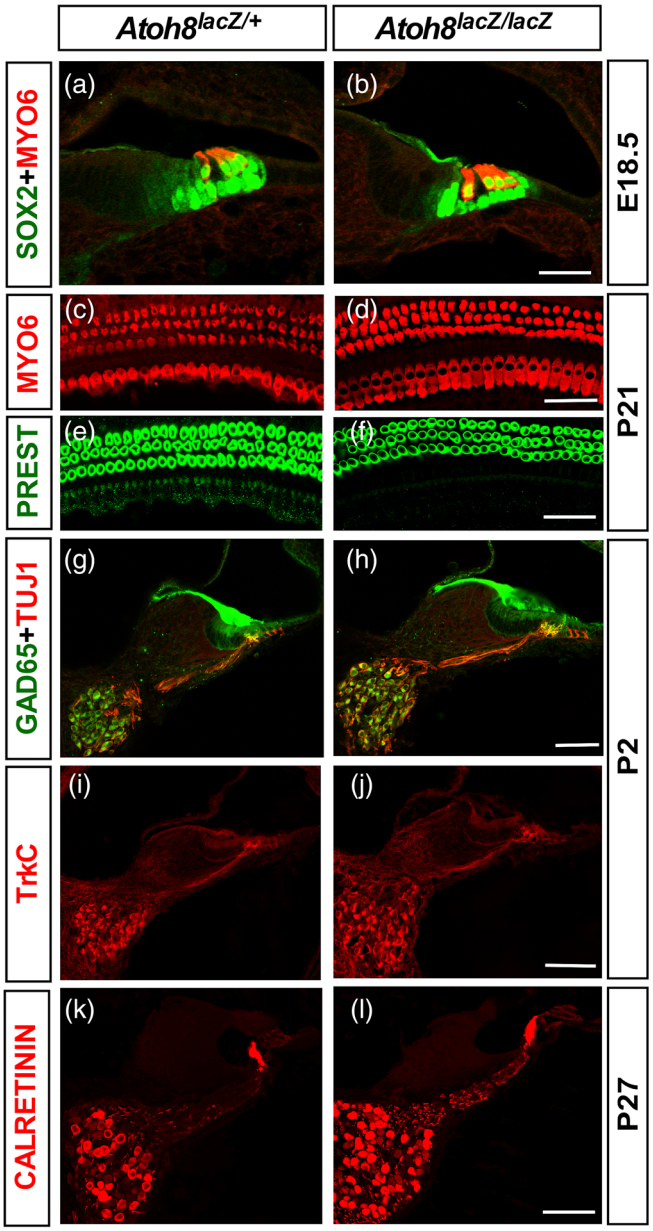

FIGURE 6 Main functional protein expression in the cochlea at later embryonic and adult stages. (a–d) "Myosin6, a marker for mature hair cells, was clearly visible in both control mouse and *Atoh8*$^{lacZ/lacZ}$ mouse cochleae. (e,f) Prestin, a marker specific for outer hair cells, was also strongly expressed in both control and mutant mice. (g–l) There seemed to be no obvious difference in the expression of TrkC, GAD65, Tuj1, or Calretinin between wild-type and mutant mice

Atoh8 in the development of the inner ear and in maintaining hearing. Atoh8 has three exons in its coding region, while Math1 and Math5 have only one exon in their coding region (Chen et al., 2011; Inoue et al., 2001). The *Atoh8*^{lacZ} knock-in allele was constructed by Dr. Lin Gan through the replacement of exon 1 with the lacZ sequence. Based on Southern blotting, PCR and RT-qPCR results, we determined that the transcription of atoh8 was completely stopped in the *atoh8* mutant mice in our study (Figure 1).

A previous report showed that Atoh8 mutant mice died at early embryonic stages (Lynn et al., 2008), while the mutant (*Atoh8*$^{lacZ/lacZ}$) mice we obtained were viable and fertile (Figure 2). One possible reason for the difference mentioned above is that exons 1 and 2 were deleted and replaced by EGFP-Cre in Lynn's report (Lynn et al., 2008), and only exon 1 was deleted and replaced by LacZ in our study.

3.2 | Atoh8 is an important gene for the maintenance of normal hearing

The clap startle test showed that the Atoh8-targeted deletion mice showed no responses to loud sound. This result suggested that Atoh8 may have important functions in hearing development or the maintenance of normal hearing.

ABR is a useful tool to study the function of the VIII cranial nerve and brainstem (Musiek, 1982). ABR is an important method to measure the objective hearing of humans and other mammals, such as mice, rats and cats. DPOAE is a noninvasive method to study the function of the outer hair cells of the inner ear and can distinguish sensory hearing loss from neural contributions (Kummer, Hotz, & Arnold, 2000; Ohlms, Lonsbury-Martin, & Martin, 1991). In our study, *Atoh8* mutant mice were severely hearing impaired. Compared to the control mice, the ABR thresholds at 8, 12, 16, 22, and 32 kHz were significantly increased in mutant mice (Figure 3a). ABR data confirmed that mutant mice were severely hearing impaired. The DPOAE thresholds at 8, 12, 16, 22, and 32 kHz were also significantly increased in mutant mice (Figure 3b), which indicates the dysfunction of outer cochlear hair cells in mutant mice. Hearing tests verified the importance of Atoh8 in maintaining normal hearing and that targeted deletion of *Atoh8* resulted in severe hearing loss.

3.3 | Possible reasons for deafness in *Atoh8* mutant mice

Multiple etiologies of deafness exist concerning the organ of Corti and spiral ganglion cells, including the deformity/dysfunction of inner and outer hair cells, the tectorial membrane, spiral ganglion neurons, and innervating nerve fibers. Our data demonstrated that the morphologies of the tectorial membrane, inner and outer hair cells and spiral ganglion cells of mutant mice were normal (Figure 7a–h). The cilia of outer hair cells of both mutant mice and control mice seemed similar under scanning EM (Figure 7i,k).

Furthermore, immunostaining data showed that Myosin6, a mature hair cell marker, was strongly expressed in the inner and outer hair cells of both mutant and control mice (Figure 7a–d). The spiral ganglion markers TUJ1, TrkC, GAD65, and Calretinin were all strongly expressed in both mutant and control mice (Figure 6g–l), which demonstrates that the function of spiral ganglion cells should be normal. The nerve fiber markers TUJ1 and Calretinin, clearly showed the

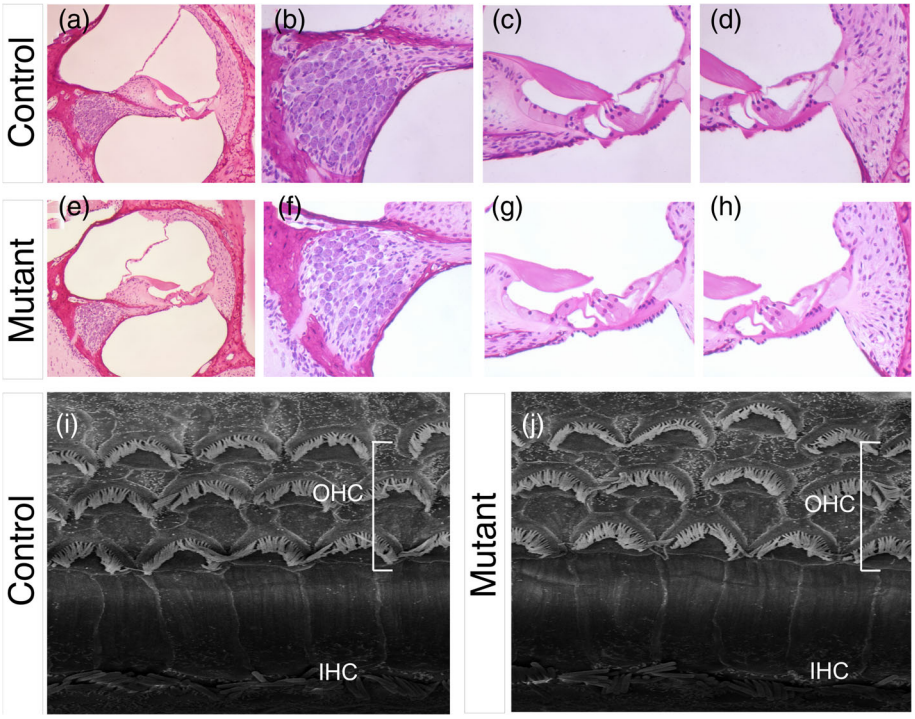

FIGURE 7 Structure of the cochlea by plastic sectioning and electron microscopy. (a–h) No obvious abnormalities in cochlear morphology, spiral ganglion cells, the organ of Corti or the tectorial membrane of mutant mice compared with control mice were observed under a light microscope. (i,j) Under scanning EM, the cilia of the inner and outer hair cells of mutant mice were clear and seemed normal compared with those of the control mice

normal development of nerve fibers innervating inner and outer hair cells (Figure 6g,h,k,l), which confirmed the normal development of innervating nerves. Immunostaining data for TrkC, a marker of the neurotransmitter-3 receptor (Urfer, Tsoulfas, O'Connell, & Presta, 1997), and GAD65, a marker of glutamate decarboxylase (Laprade & Soghomonian, 1997), also suggest the normal distribution of neurotransmitters between hair cells and spiral ganglion neurons (Figure 6g–j).

Because DPOAE measurements suggested the dysfunction of outer hair cells (OHCs) in mutant mice, we also focused on the morphology and function of outer hair cells. The morphology of outer hair cells looks normal under a light microscope in plastic sections at a thickness of 1 μm. Under scanning EM, the cilia of hair cells seemed normal (Figure 7). Because the structure of hair cells looks normal in mutant mice, we further studied the mobility function of OHCs. OHCs have a unique function of electromobility that is fulfilled by PRESTIN, the motor protein of OHCs, and necessary for cochlear amplification (Dallos et al., 2008; Liberman et al., 2002; Santos-Sacchi, Shen, Zheng, & Dallos, 2001). By wholemount cochlear immunostaining, PRESTIN was strongly detected in all the outer hair cells of both mutant and control mice at P21 (Figure 6e,f).

4 | CONCLUSIONS

Targeted deletion of Atoh8 caused severe hearing loss in mice. There seemed to be no remarkable morphological changes in the cochleae of mutant mice. Further studies are required to elucidate the exact function of Atoh8 in hearing.

5 | MATERIALS AND METHODS

5.1 | Animals

The *Atoh8*^{lacZ} allele was provided by Dr. Lin Gan. The *LacZ* coding sequence took place in exon 1, including the translational initiation codon, in *Atoh8*^{lacZ} knock-in mice under the control of *Atoh8* regulatory sequences. Heterozygous *Atoh8*$^{lacZ/+}$ mice were generated on a 129S6 and C57BL/6J mixed background as previously described (Gan, Wang, Huang, & Klein, 1999; Gan et al., 1996; Figure 1a). PCR methods were used to genotype mice from subsequent breeding of *Atoh8*$^{lacZ/+}$ heterozygotes. The PCR primers used to identify the wild-type *Atoh8* mice were Atoh8 WT-F: 5′-CGG GCC GTG GAA GAC TGT GT-3′ and Atoh8 WT-R: 5′-CGA GAG GCG CGG ATT GTG-3′. The PCR primers used to identify the *lacZ* knock-in allele were Atoh8-F: 5′-CGG GCG GCG CTG AGT GA-3′ and lacZ KI-R: 5′-TGG CGA AAG GGG GAT GTG CT-3′.

Embryonic day 0.5 (E0.5) was defined as the day when the vaginal plug was detected. The Committee of Animal Resources of PUMC Hospital and University Committee of Animal Resources at the University of Rochester approved all animal procedures described here. The mouse strains were maintained in the C57BL/6J and 129S6 mixed background.

5.2 | Real time qPCR validation

Total RNAs were extracted by using RNeasy Mini kit (Qiagen, #74104) according to manufacturer's instruction. Extracted RNA from mice inner ear, eye and kidney, respectively, was reversely transcribed

to synthesize cDNA for RT-qPCR analysis by using iScript cDNA Synthesis Kit (BIO-RAD, #170-8890) following the manufacturer's instruction. RT-qPCR was performed following the SsoAdvanced Universal SYBR Green Supermix (BIO-RAD, #1725271) manufacturer's instruction. The $2^{-\Delta\Delta Ct}$ method was used to determine the relative expression level of mRNA.

5.3 | Auditory brainstem response (ABR) and distortion product Otoacoustic emission (DPOAE) measurement

The measurement procedures of ABR and DPOAE were similar to the methods reported previously (Frisina, Newman, & Zhu, 2007; Zhu et al., 2007). ABRs were measured in mice sedated with acepromazine (10 mg/kg i.p.) and ketamine (100 mg/kg i.p.). Needle electrodes were inserted at the vertex (noninverted) and in the muscle posterior to the pinna (inverted), with a ground inserted under the contralateral pinna. ABR waveforms were evoked with 5-ms tone pips (0.5-ms rise-fall times) with a $\cos^2$ onset envelope, delivered at 29/s through a high-frequency leaf tweeter (Panasonic 100THD) placed 20 cm from the left pinna. The response was amplified (×10,000), filtered (100 Hz–3 kHz), and averaged using the BioSig (TDT, Gainesville, FL) data-acquisition system. A total of 200 responses were averaged (with stimulus polarity alternated) using an "artifact reject", whereby response waveforms were discarded when the peak-to-peak amplitude exceeded 7 μV to prevent contamination by muscle and cardiac activities. Intensity was varied in 5 dB steps and decreased to at least 20 dB below the threshold for the specific test frequency. Each intensity was replicated, and the threshold was defined as the lowest intensity at which a response was replicated.

DPOAE amplitudes were measured in the following manner. Two primaries (F1 and F2) were generated at 65 and 50 dBSPL, respectively. The ratio of the two frequencies was 1.25, and the frequencies were based on geometric mean frequencies ranging from 5.6 to 44.8 kHz. Waveforms of the output of the ER10B+ probe microphone were captured on a TDT RP2.1. FFTs for each presentation were averaged together, and the signal level at five frequencies was sampled: F1, F2, DP (2F1-F2), and two noise bins above and below the DP frequency. Following FFT sampling, dBV was converted to SPL based on the ER10B+ microphone calibration. The DPOAE threshold was defined as the F1 level required to produce a DP of 0 dB SPL (±1 dB). The identification of thresholds required two successive trials of F1 and F2 levels that evoked a 0 dB SPL DP amplitude.

5.4 | Immunohistochemistry, in situ hybridization, and X-Gal staining

Staged embryos and tissue samples were dissected and immediately fixed in 4% paraformaldehyde (PFA) in PBS for 1–2 hr. The samples were then embedded and frozen in OCT compound (TissueTek) for cryosections.

For immunohistochemistry staining, cryosections were cut at a thickness of 18 μm. The working dilutions and sources of antibodies used in this study were chicken anti-LacZ (1:500, Abcam #ab9361-250), rabbit anti-MYO6 (1:500, Proteus Biosciences Inc., #25–6,791), goat anti-SOX2 (1:500, Santa Cruz# SC-17320), goat anti-PRESTIN (1:200, Santa Cruz, sc-22,692), rabbit anti-GAD65 (1:200, Chemicon # AB5082), goat anti-TrkC (1:100, R&D System # AF1404), rabbit anti-Calretinin (1:2000, Oncogene # PC254L), and rabbit anti-ß-tubulin (1:500, Covance #PRB-435P). Alexa-conjugated secondary antibodies (Molecular Probes) were used at a concentration of 1:1,000. Immunolabeled sections were scanned and photographed under a Zeiss LSM 510 META confocal microscope.

For in situ hybridization experiments, samples were cryosectioned at 20 μm thickness and treated as previously described (Li & Joyner, 2001).

The detection of *lacZ* expression was determined by X-Gal staining (Gan et al., 1996; Gan et al., 1999). Briefly, cryosections were prepared at a thickness of 20 μm and stained at 30°C overnight in 1 mg/ml X-Gal, 4 mM $K_4Fe(CN)_6$, 4 mM $K_3Fe(CN)_6$, and 2 mM $MgCl_2$ in PBS. For wholemount X-Gal staining, embryos were fixed in 4% PFA in PBS overnight and stained at 30°C overnight in the staining solution.

5.5 | Electron microscopy

Cochlear samples were fixed and decalcified and then embedded in plastic. Plastic samples were sectioned at a thickness of 1 μm and stained with hematoxylin and eosin.

For scanning electron microscopy (SEM), adult mice were perfused with EM fixatives (6% glutaraldehyde in 0.1 M cacodylate buffer with 1 mM $CaCl_2$) (Elshatory et al., 2007), and cochleae were dissected out quickly and fixed in EM fixative overnight. Cochlear samples were then rinsed with EM Buffer (0.1 M sodium cacodylate) and placed in decalcification buffer (10% EDTA solution containing 1.0% glutaraldehyde in EM buffer) for 3–4 days. The procedures for SEM were similar to the methods reported previously (Mizuta, Hoshino, & Morita, 1990; Voelker, Henderson, Macklin, & Tucker, 1980).

ACKNOWLEDGMENTS

The authors thank Dr. Lin Gan and the members of the Gan Laboratory for their helpful discussions and technical assistance. This study was supported by the National Natural Science Foundation of China (grant number 81470698) to Hua Yang; the Beijing Natural Science Foundation (grant number 7172176) to Hua Yang; and the Scientific Project of Young and Middle-aged Researchers of PUMCH (grant number pumch-2013-007) to Hua Yang.

AUTHOR CONTRIBUTIONS

Conceived and designed the experiments: Hua Yang. Performed the experiments: Qi Tang, Meng-Yao Xie, and Hua Yang. Analyzed

the data: Qi Tang, Meng-Yao Xie, Yong-Li Zhang, and Hua Yang. Contributed reagents/materials/analysis tools: Ruo-Yan Xue and Xiao-Hui Zhu. Wrote the paper: Hua Yang, Qi Tang and Meng-Yao Xie.

DATA AVAILABILITY STATEMENT

The data that support the findings of this study are available from the corresponding author upon reasonable request.

ORCID

Qi Tang https://orcid.org/0000-0002-0959-1295

REFERENCES

Alvarez, Y., Alonso, M. T., Vendrell, V., Zelarayan, L. C., Chamero, P., Theil, T., … Schimmang, T. (2003). Requirements for FGF3 and FGF10 during inner ear formation. *Development*, *130*(25), 6329–6338. https://doi.org/10.1242/dev.00881

Bermingham, N. A., Hassan, B. A., Price, S. D., Vollrath, M. A., Ben-Arie, N., Eatock, R. A., … Zoghbi, H. Y. (1999). Math1: An essential gene for the generation of inner ear hair cells. *Science*, *284*(5421), 1837–1841. https://doi.org/10.1126/science.284.5421.1837

Chen, J., Balakrishnan-Renuka, A., Hagemann, N., Theiss, C., Chankiewitz, V., Chen, J., … Brand-Saberi, B. (2016). A novel interaction between ATOH8 and PPP3CB. *Histochemistry and Cell Biology*, *145*(1), 5–16. https://doi.org/10.1007/s00418-015-1368-5

Chen, J., Dai, F., Balakrishnan-Renuka, A., Leese, F., Schempp, W., Schaller, F., … Brand-Saberi, B. (2011). Diversification and molecular evolution of ATOH8, a gene encoding a bHLH transcription factor. *PLoS One*, *6*(8), e23005. https://doi.org/10.1371/journal.pone.0023005

Chen, P., Johnson, J. E., Zoghbi, H. Y., & Segil, N. (2002). The role of Math1 in inner ear development: Uncoupling the establishment of the sensory primordium from hair cell fate determination. *Development*, *129*(10), 2495–2505.

Dallos, P., Wu, X., Cheatham, M. A., Gao, J., Zheng, J., Anderson, C. T., … Zuo, J. (2008). Prestin-based outer hair cell motility is necessary for mammalian cochlear amplification. *Neuron*, *58*(3), 333–339. https://doi.org/10.1016/j.neuron.2008.02.028

Ejarque, M., Altirriba, J., Gomis, R., & Gasa, R. (2013). Characterization of the transcriptional activity of the basic helix-loop-helix (bHLH) transcription factor Atoh8. *Biochimica et Biophysica Acta*, *1829*(11), 1175–1183. https://doi.org/10.1016/j.bbagrm.2013.08.003

Ejarque, M., Mir-Coll, J., Gomis, R., German, M. S., Lynn, F. C., & Gasa, R. (2016). Generation of a conditional allele of the transcription factor atonal homolog 8 (Atoh8). *PLoS One*, *11*(1), e0146273. https://doi.org/10.1371/journal.pone.0146273

Elshatory, Y., Everhart, D., Deng, M., Xie, X., Barlow, R. B., & Gan, L. (2007). Islet-1 controls the differentiation of retinal bipolar and cholinergic amacrine cells. *The Journal of Neuroscience*, *27*(46), 12707–12720. https://doi.org/10.1523/jneurosci.3951-07.2007

Feng, L., Xie, Z. H., Ding, Q., Xie, X., Libby, R. T., & Gan, L. (2010). MATH5 controls the acquisition of multiple retinal cell fates. *Molecular Brain*, *3*, 36. https://doi.org/10.1186/1756-6606-3-36

Frisina, R. D., Newman, S. R., & Zhu, X. (2007). Auditory efferent activation in CBA mice exceeds that of C57s for varying levels of noise. *The Journal of the Acoustical Society of America*, *121*(1), EI29–EI34. https://doi.org/10.1121/1.2401226

Fritzsch, B., Matei, V. A., Nichols, D. H., Bermingham, N., Jones, K., Beisel, K. W., & Wang, V. Y. (2005). Atoh1 null mice show directed afferent fiber growth to undifferentiated ear sensory epithelia followed by incomplete fiber retention. *Developmental Dynamics*, *233*(2), 570–583. https://doi.org/10.1002/dvdy.20370

Gan, L., Wang, S. W., Huang, Z., & Klein, W. H. (1999). POU domain factor Brn-3b is essential for retinal ganglion cell differentiation and survival but not for initial cell fate specification. *Developmental Biology*, *210*(2), 469–480. https://doi.org/10.1006/dbio.1999.9280

Gan, L., Xiang, M., Zhou, L., Wagner, D. S., Klein, W. H., & Nathans, J. (1996). POU domain factor Brn-3b is required for the development of a large set of retinal ganglion cells. *Proceedings of the National Academy of Sciences of the United States of America*, *93*(9), 3920–3925. https://doi.org/10.1073/pnas.93.9.3920

Inoue, C., Bae, S. K., Takatsuka, K., Inoue, T., Bessho, Y., & Kageyama, R. (2001). Atoh8, a bHLH gene expressed in the developing nervous system, regulates neuronal versus glial differentiation. *Genes to Cells*, *6*(11), 977–986. https://doi.org/10.1046/j.1365-2443.2001.00476.x

Jahan, I., Pan, N., Kersigo, J., & Fritzsch, B. (2010). Neurod1 suppresses hair cell differentiation in ear ganglia and regulates hair cell subtype development in the cochlea. *PLoS One*, *5*(7), e11661. https://doi.org/10.1371/journal.pone.0011661

Kiernan, A. E., Pelling, A. L., Leung, K. K., Tang, A. S., Bell, D. M., Tease, C., … Cheah, K. S. (2005). Sox2 is required for sensory organ development in the mammalian inner ear. *Nature*, *434*(7036), 1031–1035. https://doi.org/10.1038/nature03487

Kim, W. Y., Fritzsch, B., Serls, A., Bakel, L. A., Huang, E. J., Reichardt, L. F., … Lee, J. E. (2001). NeuroD-null mice are deaf due to a severe loss of the inner ear sensory neurons during development. *Development*, *128*(3), 417–426.

Kummer, P., Hotz, M. A., & Arnold, W. (2000). Assessment of outer hair cell function recovery by means of the DPOAE threshold. *Schweizerische Medizinische Wochenschrift*, (suppl 125), 77s–79s.

Laprade, N., & Soghomonian, J. J. (1997). Glutamate decarboxylase (GAD65) gene expression is increased by dopamine receptor agonists in a subpopulation of rat striatal neurons. *Brain Research. Molecular Brain Research*, *48*(2), 333–345. https://doi.org/10.1016/s0169-328x(97)00112-5

Lawoko-Kerali, G., Rivolta, M. N., Lawlor, P., Cacciabue-Rivolta, D. I., Langton-Hewer, C., van Doorninck, J. H., & Holley, M. C. (2004). GATA3 and NeuroD distinguish auditory and vestibular neurons during development of the mammalian inner ear. *Mechanisms of Development*, *121*(3), 287–299. https://doi.org/10.1016/j.mod.2003.12.006

Li, H., Corrales, C. E., Wang, Z., Zhao, Y., Wang, Y., Liu, H., & Heller, S. (2005). BMP4 signaling is involved in the generation of inner ear sensory epithelia. *BMC Developmental Biology*, *5*, 16. https://doi.org/10.1186/1471-213x-5-16

Li, J. Y., & Joyner, A. L. (2001). Otx2 and Gbx2 are required for refinement and not induction of mid-hindbrain gene expression. *Development*, *128*(24), 4979–4991.

Liberman, M. C., Gao, J., He, D. Z., Wu, X., Jia, S., & Zuo, J. (2002). Prestin is required for electromotility of the outer hair cell and for the cochlear amplifier. *Nature*, *419*(6904), 300–304. https://doi.org/10.1038/nature01059

Lynn, F. C., Sanchez, L., Gomis, R., German, M. S., & Gasa, R. (2008). Identification of the bHLH factor Atoh8 as a novel component of the embryonic pancreas transcriptional network. *PLoS One*, *3*(6), e2430. https://doi.org/10.1371/journal.pone.0002430

Matei, V., Pauley, S., Kaing, S., Rowitch, D., Beisel, K. W., Morris, K., … Fritzsch, B. (2005). Smaller inner ear sensory epithelia in Neurog 1 null mice are related to earlier hair cell cycle exit. *Developmental Dynamics*, *234*(3), 633–650. https://doi.org/10.1002/dvdy.20551

Mizuta, K., Hoshino, T., & Morita, H. (1990). Scanning electron microscopy of the celloidin-embedded inner ear sections. *Scanning Microscopy*, *4*(4), 967–972 discussion 973.

Musiek, F. E. (1982). ABR in eighth-nerve and brain-stem disorders. *The American Journal of Otology*, *3*(3), 243–248.

Oesterle, E. C., Campbell, S., Taylor, R. R., Forge, A., & Hume, C. R. (2008). Sox2 and JAGGED1 expression in normal and drug-damaged adult

mouse inner ear. *Journal of the Association for Research in Otolaryngology*, *9*(1), 65–89. https://doi.org/10.1007/s10162-007-0106-7

Ohlms, L. A., Lonsbury-Martin, B. L., & Martin, G. K. (1991). Acoustic-distortion products: Separation of sensory from neural dysfunction in sensorineural hearing loss in human beings and rabbits. *Otolaryngology and Head and Neck Surgery*, *104*(2), 159–174. https://doi.org/10.1177/019459989110400203

Place, E. S., & Smith, J. C. (2017). Zebrafish atoh8 mutants do not recapitulate morpholino phenotypes. *PLoS One*, *12*(2), e0171143. https://doi.org/10.1371/journal.pone.0171143

Raft, S., Koundakjian, E. J., Quinones, H., Jayasena, C. S., Goodrich, L. V., Johnson, J. E., … Groves, A. K. (2007). Cross-regulation of Ngn1 and Math1 coordinates the production of neurons and sensory hair cells during inner ear development. *Development*, *134*(24), 4405–4415. https://doi.org/10.1242/dev.009118

Rawnsley, D. R., Xiao, J., Lee, J. S., Liu, X., Mericko-Ishizuka, P., Kumar, V., … Kahn, M. L. (2013). The transcription factor atonal homolog 8 regulates Gata4 and friend of Gata-2 during vertebrate development. *The Journal of Biological Chemistry*, *288*(34), 24429–24440. https://doi.org/10.1074/jbc.M113.463083

Ross, M. D., Martinka, S., Mukherjee, A., Sedor, J. R., Vinson, C., & Bruggeman, L. A. (2006). Atoh8 expression during kidney development and altered expression in a mouse model of glomerulosclerosis. *Developmental Dynamics*, *235*(11), 3102–3109. https://doi.org/10.1002/dvdy.20934

Santos-Sacchi, J., Shen, W., Zheng, J., & Dallos, P. (2001). Effects of membrane potential and tension on prestin, the outer hair cell lateral membrane motor protein. *The Journal of Physiology*, *531*(Pt 3), 661–666. https://doi.org/10.1111/j.1469-7793.2001.0661h.x

Urfer, R., Tsoulfas, P., O'Connell, L., & Presta, L. G. (1997). Specificity determinants in neurotrophin-3 and design of nerve growth factor-based trkC agonists by changing central beta-strand bundle residues to their neurotrophin-3 analogs. *Biochemistry*, *36*(16), 4775–4781. https://doi.org/10.1021/bi962877+

Voelker, F. A., Henderson, C. M., Macklin, A. W., & Tucker, W. E. (1980). Evaluating the rat inner ear. A technique using scanning electron microscopy. *Archives of Otolaryngology*, *106*(10), 613–617. https://doi.org/10.1001/archotol.1980.00790340021005

Wang, B., Balakrishnan-Renuka, A., Napirei, M., Theiss, C., & Brand-Saberi, B. (2015). Spatiotemporal expression of Atoh8 during mouse embryonic development. *Histochemistry and Cell Biology*, *143*(6), 575–582. https://doi.org/10.1007/s00418-014-1305-z

Wang, S. W., Kim, B. S., Ding, K., Wang, H., Sun, D., Johnson, R. L., … Gan, L. (2001). Requirement for math5 in the development of retinal ganglion cells. *Genes & Development*, *15*(1), 24–29. https://doi.org/10.1101/gad.855301

Wang, Z., Xie, J., Yan, M., Wang, J., Wang, X., Zhang, J., … Liu, Q. (2016). Downregulation of ATOH8 induced by EBV-encoded LMP1 contributes to the malignant phenotype of nasopharyngeal carcinoma. *Oncotarget*, *7*(18), 26765–26779. https://doi.org/10.18632/oncotarget.8503

Wright, T. J., & Mansour, S. L. (2003). FGF signaling in ear development and innervation. *Current Topics in Developmental Biology*, *57*, 225–259. https://doi.org/10.1016/s0070-2153(03)57008-9

Yang, Z., Ding, K., Pan, L., Deng, M., & Gan, L. (2003). Math5 determines the competence state of retinal ganglion cell progenitors. *Developmental Biology*, *264*(1), 240–254. https://doi.org/10.1016/j.ydbio.2003.08.005

Yao, J., Zhou, J., Liu, Q., Lu, D., Wang, L., Qiao, X., & Jia, W. (2010). Atoh8, a bHLH transcription factor, is required for the development of retina and skeletal muscle in zebrafish. *PLoS One*, *5*(6), e10945. https://doi.org/10.1371/journal.pone.0010945

Zhang, Y., Tang, Q., Xue, R., Gao, J., Yang, H., Gao, Z., & Lin, G. (2018). Absence of Atoh1 induced partially different cell fates of cochlear and vestibular sensory epithelial cells in mice. *Acta Oto-Laryngologica*, *138*(11), 972–976. https://doi.org/10.1080/00016489.2018.1497855

Zhu, X., Vasilyeva, O. N., Kim, S., Jacobson, M., Romney, J., Waterman, M. S., … Frisina, R. D. (2007). Auditory efferent feedback system deficits precede age-related hearing loss: Contralateral suppression of otoacoustic emissions in mice. *The Journal of Comparative Neurology*, *503*(5), 593–604. https://doi.org/10.1002/cne.21402

How to cite this article: Tang, Q., Xie, M.-Y., Zhang, Y.-L., Xue, R.-Y., Zhu, X.-H., & Yang, H. (2021). Targeted deletion of *Atoh8* results in severe hearing loss in mice. *genesis*, *59*(9), e23442. https://doi.org/10.1002/dvg.23442